Crystal growth of aragonite in the presence of phosphate

Solene Tadier, Stamatia Rokidi, Christian Rey, Christèle Combes, Petros G. Koutsoukos

Crystal growth of aragonite in the presence of phosphate

Solène Tadier[a,1], Stamatia Rokidi[b], Christian Rey[a], Christèle Combes[a,*], Petros G. Koutsoukos[b]

[a] CIRIMAT, University of Toulouse, CNRS, INPT, UPS, ENSIACET, 4 allée Emile Monso, CS 44362, 31030 Toulouse cedex 4, France
[b] University of Patras, Department of Chemical Engineering and FORTH-ICEHT, Patras, Greece

ARTICLE INFO

Communicated by Dr. T.F. Kuech

Keywords:
A1. Biocrystallization
A2. Growth from solutions
A1. adsorption
A1. Characterization
B1. Inorganic compounds
B1. Phosphates

ABSTRACT

The crystal growth of aragonite was investigated at pH 7.8, 37 °C and constant solution supersaturation from aragonite-seeded supersaturated solutions. The effect of the presence of orthophosphate ions in the supersaturated solution on the kinetics of crystallization of aragonite was investigated over the range of orthophosphate concentrations of 0.25 μM–1 mM. In the presence of orthophosphate in the range of 0.25 μM–8 μM, the crystal growth rate of aragonite decreased with increasing phosphate concentration. At orthophosphate concentration levels exceeding 2 μM, induction times were measured and were found to increase with orthophosphate concentration. At orthophosphate concentration levels > 8 μM, the crystal growth of aragonite was inhibited, suggesting the blockage of the active growth sites by the adsorption of orthophosphate ions. Adsorption was confirmed by the investigation of orthophosphate uptake on aragonite, which was: i) found to depend on the equilibrium concentration of orthophosphate in aqueous solutions saturated with respect to aragonite; ii) not influenced by the ionic strength of the electrolyte up to 0.15 M NaCl, showing that electrostatic interactions between orthophosphate and $CaCO_3$ did not play a significant role in this concentration range. Adsorption data of orthophosphate on the aragonite crystals gave satisfactory fit to the Langmuir adsorption model and was confirmed by XPS analysis.

1. Introduction

Calcium carbonate exists in six polymorphic forms: calcite (thermodynamically the most stable), aragonite, vaterite, amorphous $CaCO_3$, and two hydrated crystalline phases, calcium carbonate monohydrate and hexahydrate. Precipitation, crystallization and dissolution of calcium carbonate species have been intensively studied over the past decades because of the significance of these processes in the formation of scale or deposits, in biological mineralization and in various environmental conditions [1,2].

The presence of foreign substances in the supersaturated fluid media in which growth of calcium carbonate polymorphs takes place may interfere with the crystal growth process because of the interactions of these substances with the lattice ions of calcium carbonate at the respective active crystal growth sites [3,4]. Early investigations have shown that very low phosphate concentrations decreased the rates of calcite precipitation [5,6]. The inhibition effect was attributed to the competition between carbonate and phosphate ions to bind to the available calcium ions. Katsifaras and Spanos [7] have found that vaterite was stabilized in the presence of low phosphate concentrations and that its growth rate was reduced at the same time. This was attributed to the adsorption of the orthophosphate ions on vaterite crystals. Evidence concerning the adsorption of orthophosphate has been reported from dissolution studies of calcium carbonate polymorphs [8]. In addition, the presence of orthophosphate in solutions supersaturated with respect to the calcium carbonate, in combination with pH, has been suggested to play a key role in the stabilization of less stable polymorphs [9]. Environmental studies concerned with the interaction of carbonates and phosphates have quantified the interaction between inorganic orthophosphate and calcite and aragonite mineral surfaces [10–14]. Studies on the interaction of calcium carbonate with phosphate by Stumm and Leckie [15] suggested that the uptake of phosphorus is a complex process consisting of chemisorption and surface precipitation of calcium phosphates. Millero et al. [16] has reported large extents of uptake and desorption of phosphate on aragonite surfaces, which were suppressed in the presence of seawater. It has also been claimed from reports in literature that phosphate is chemisorbed on calcium carbonate substrates and would become less susceptible to electrostatic forces [17]. Both studies pointed out the role of the ionic strength on the orthophosphate-

* Corresponding author.
E-mail addresses: solene.tadier@insa-lyon.fr (S. Tadier), srokidi@chemeng.upatras.gr (S. Rokidi), christian.rey@ensiacet.fr (C. Rey), christele.combes@ensiacet.fr (C. Combes), pgk@chemeng.upatras.gr (P.G. Koutsoukos).
[1] Present address: Univ. Lyon, INSA Lyon, MATEIS CNRS UMR5510, 69621 Villeurbanne, France.

http://dx.doi.org/10.1016/j.jcrysgro.2016.10.046

carbonate interaction.

The need of biomaterials for the replacement or healing of damaged bone tissues has been one of the driving force for the development of materials based on calcium carbonate, particularly those of marine origin that have been shown to be biocompatible and bioactive [18,19]. Calcium carbonate based cements have been proposed and shown to be effective biomaterials [20–22] and aragonite has been presented as a promising implant material [23]. The presence of inorganic orthophosphate in the body fluids in contact with calcium carbonate is believed to play an important role for the ability of $CaCO_3$ polymorphs to act efficiently as biomaterials. In particular, their *in vivo* evolution and resorption behavior will most probably be impacted by the presence of these orthophosphate ions [24].

Concerning the effect of the presence of orthophosphate on the kinetics of crystal growth of aragonite, a limited number of studies have been conducted under conditions in which the chemistry of the supersaturated solutions was maintained relatively constant, although limitations concerning the concentrations [25–27] or the establishment of steady state conditions past an initial rapid de-supersaturation of the solutions have been applied [28].

In this study, a highly reproducible seeded growth technique is employed to investigate the crystallization of aragonite crystals in presence and absence of orthophosphate ions. The investigation was done under conditions of constant supersaturation, achieved by the addition of titrant solutions in which the concentrations have been calculated appropriately, to ensure replacement of the ions transferred from the supersaturated solutions to the crystallizing solid, ensuring that the interaction of orthophosphate ions during the growth was not disturbed by factors such as the solution de-supersaturation. Moreover, the adsorption of orthophosphate on aragonite crystals was quantified by equilibrium studies and interpretation according to the Langmuir isotherm.

2. Materials and methods

2.1. Synthesis of aragonite seed crystals

Aragonite seeds were prepared by precipitation at 100 °C. Briefly, 0.1 M $CaCl_2{\cdot}2H_2O$ (Normapur) solution was added dropwise into 0.1 M Na_2CO_3 (Normapur) solution containing 1 mM $SrCO_3$ (Alfa Aesar). The formed precipitate was filtered through membrane filters, washed with 1 L of deionized water, freeze-dried and stored in a freezer to prevent any evolution of aragonite before use. The specific surface area of the synthesized aragonite seed crystals was measured in triplicate using a multiple point BET apparatus and was equal to 3.0 $m^2\ g^{-1}$.

2.2. Characterization of aragonite crystals

Aragonite seeds and grown crystals were characterized by FTIR spectroscopy (Nicolet 5700 spectrometer, ThermoElectron), X-ray diffraction (XRD, Inel CPS 120 diffractometer – with a Co anticathode, λ=1.78897 Å), and scanning electron microscopy (SEM, LEO 435 VP and FEI QUANTA FEG microscopes, samples were silver-plated before observation).

2.3. Crystal growth experiments at constant composition

All solutions were freshly prepared using analytical reagent grade chemicals without further purification, dissolved in triply distilled CO_2-free water, and were filtered (0.45 μM Millipore® filters) before use. Supersaturated solutions were prepared using $CaCl_2{\cdot}2H_2O$ (Ferrak Berlin), $NaHCO_3$ (Merck) and NaCl (Merck) salts. The supersaturated solutions (200 mL) were prepared into a double walled, water jacketed glass reactor. The reactor was kept at 37 ± 0.1 °C by circulating water from a thermostat. The reactor was tightly sealed and a light stream of nitrogen gas was passed above the solution to prevent intrusion of atmospheric CO_2. The pH of the supersaturated solutions was adjusted by the addition of standard sodium hydroxide or hydrochloric acid solutions as needed. The pH was monitored by a pH-meter (Metrohm®) and the electrode was calibrated before and after the experiments with NIST standard buffer solutions at pH 6.84 and 7.38. During the course of crystal growth, the concomitant pH drop triggered the addition of titrant solutions including calcium and carbonate concentrations that were calculated appropriately to counter-balance the ions removed from the supersaturated solution during aragonite crystallization.

During equilibration the solution pH remained constant, thus confirming the stability of the supersaturated solutions. After equilibrium was attained, an accurately weighted amount of aragonite seed crystals (40 mg) was introduced in the supersaturated solution, triggering the initiation of crystal growth of the aragonite seed crystals. For the experiments in the presence of inorganic orthophosphate ions, Na_2HPO_4 (Merck) was dissolved in the initial supersaturated solutions to obtain orthophosphate concentrations in the range of 0.25–1 mM. No orthophosphate was added into titrant solutions; therefore, there was no compensation for possible phosphate consumption during the experiments. Preliminary work showed that adsorption of phosphate on calcium carbonate was very fast and thus no pre-equilibration of the seed crystals was necessary before starting the experiment.

The formation of aragonite in the supersaturated solutions may be described by Eq. (1):

$$Ca^{2+}(aq)+x\ H_2CO_3(aq)+y\ HCO_3^-(aq)+u\ CO_3^{2-}(aq)\rightarrow CaCO_3\ (arag{\cdot},\ s)+z\ H^+(aq) \quad (1)$$

where 2x+y=z

As may be seen from Eq. (1) protons are released during the crystallization process. A drop in the pH as small as 0.005 pH units triggered the addition of titrant solutions from two mechanically coupled syringes of a computer controlled automatic titrator. The titrants and the corresponding concentrations in the two syringes were calculated as shown in Eqs. (2) and (3):

$$Ca_T=10\ Ca_s+2\ Ca_s \quad (2)$$

$$C_T=10\ C_s+2C_s+2(C_A,\ C_B) \quad (3)$$

where Ca_T is total calcium in the titrant solution and Ca_s the respective concentration in the supersaturated solution. C_T is the concentration of the total carbonate in the titrant solution and C_s the corresponding concentration in the supersaturated solution. C_A and C_B are the concentrations of standard acid or base, respectively, added to adjust the pH of the supersaturated solutions at the desired value. The compositions of the two titrant solutions were calculated so that their addition ensured the constancy not only of the solution pH but also of the activity of all ions present in the supersaturated solutions. Eq. (2) consists of two parts: $10Ca_s$ is an arbitrarily selected concentration, based on preliminary experiments. This part corresponds to the calcium added to compensate calcium precipitating as calcium carbonate. The value used for this part, was selected on the basis of the optimum value to avoid variations of the calcium concentration in solution greater than 1%. If this factor is too high the titrant volume-time curves show extended steps and if it is too low, it is impossible for the titrants to compensate for the formation of precipitates. The second part of Eq. (2) refers to the amount of titrants needed to avoid dilution of the initial calcium concentration in the solution. Eq. (3), gives the concentration of the titrant solution used for the compensation of carbonate going to the precipitate. The first term corresponds to the concentration needed to keep carbonate constant in solution through the replacement of the precipitating carbonate and the second term is to account for the dilution of the initial supersaturated solution. The third term in Eq. (3) accounts for the acid/base concentration needed to adjust the solution pH to the desired value. Having additions from

two syringes, in order to maintain the initial solution concentrations, all related concentrations are multiplied by two. All experiments were done at constant ionic strength 0.15 M NaCl.

Samples were withdrawn during the course of crystallization, filtered through membrane filters and the filtrates were analyzed for calcium concentration, in order to ensure the constancy of the solution composition. The solid samples were also collected after filtration and washing, dried in a desiccator and then analyzed by FTIR spectroscopy and scanning electron microscopy. The rates of crystal growth were directly calculated from the slope of the linear graphs of the volume of titrant solutions added as a function of time. As may be seen from equations (2) and (3) the volume of titrants added, V, as a function of time, t, corresponds to the mass of $CaCO_3$ precipitating (titrants replace the precipitating ions). Since the stoichiometry of calcium: carbonate in the solid is 1:1, added calcium is equal to carbonate and the moles of calcium carbonate precipitating per unit time are easily calculated. The rates of crystal growth, R_g, were calculated as follows:

$$R_g = \frac{(\frac{dV}{dt})_\tau}{\tau \times m_s \times SSA} \quad (4)$$

In Eq. (4), the slope dV/dt of the titrant volume-time profile was taken at a given time, τ, which corresponded by relatively early stages of crystal growth, to avoid changes of the solid's surface area, m_s, was the mass of the seed crystals used and SSA the corresponding specific surface area (measured using BET method).

2.4. Adsorption study

To study the adsorption of orthophosphate ions on aragonite crystals, accurately weighted amounts of aragonite seed crystals were suspended in solutions saturated with respect to aragonite. The concentration of orthophosphate ions in each test solution was adjusted by the addition of a stock solution of NaH_2PO_4, as needed, to make up concentrations over the range between 2.5 μM and 10 μM. The pH of the suspension was adjusted at 8.2 by the addition of standard sodium hydroxide solution. A series of adsorption measurements were carried out for three different ionic strengths: in distilled water (no NaCl), and for ionic strength of 0.01 M and 0.15 M (adjusted with NaCl). The aragonite suspensions were prepared in 50 mL stoppered tubes which were rotated end over end for a period of 24 h at 25 °C to ensure establishment of equilibrium. Preliminary measurements showed that adsorption was complete (> 95%) within the first 5 min and that between 10 h and up to 48 h no further change was found, in agreement with literature reports in which this fast uptake is attributed to adsorption [29]. Following equilibration, the aqueous phase was separated from the solid residue and was analyzed spectrophotometrically for phosphate at λ=420 nm using the vanadomolybdate complex method.

Further analyses of the aragonite surfaces equilibrated with orthophosphate were done using X-ray photoelectron spectroscopy (XPS) in order to analyze the very first surface layers of the aragonite crystals. The photoemission experiments were carried out in an ultra-high vacuum system (UHV), which consisted of a fast entry specimen assembly, a sample preparation and an analysis chamber. The pressure in both chambers was 1×10^{-9} mbar. The unmonochromatized MgKα line at 1253.6 eV and an analyzer pass energy of 97 eV, giving a full width at half maximum (FWHM) of 1.7 eV for the Au $4f_{7/2}$ peak, were used in all XPS measurements. The samples were either pressed on foil or into pellets.

The reversibility of adsorption was investigated by equilibrating the aragonite crystals after adsorption and washing with phosphate free solutions saturated with regard to aragonite and of the same ionic strength as in the case of adsorption. The equilibration time allowed for the desorption process was extended over a period of one week because, in general, desorption is significantly slower than adsorption.

3. Results and discussion

3.1. Influence of solution supersaturation on aragonite crystallization in the absence of orthophosphate ions

The thermodynamic driving force for crystallization of aragonite on the aragonite seeds is the change in Gibbs free energy, ΔG, for going from the supersaturated solution to equilibrium:

$$\Delta G = -RT \ln \frac{(\alpha_{Ca^{2+}})_s(\alpha_{CO_3^{2-}})_s}{(\alpha_{Ca^{2+}})_\infty(\alpha_{CO_3^{2-}})_\infty} = -RT \ln \left\{ \frac{(\alpha_{\pm,CaCO_3})_s}{(\alpha_{\pm,CaCO_3})_\infty} \right\}^{\frac{1}{2}} = -\frac{RT}{2} \ln \frac{IAP}{K_s^0} \quad (5)$$

In Eq. (5), subscripts *s* and ∞ refer to the supersaturated solutions and at equilibrium respectively, *α* are the activities of the subscripted ions and ± denotes mean ion activity coefficients. IAP is the ion activity product of the respective solid and $K_s{}^0$ the thermodynamic solubility product of the considered phase. Ω is the saturation ratio with respect to the solid phase considered, and is defined as:

$$\Omega = \frac{IAP}{K_s^0} \quad (6)$$

The activities of all ionic species in the supersaturated solutions were calculated using PHREEQC software [30]. The relative supersaturation, σ, is given by:

$$\sigma = \left(\frac{IAP}{K_s^0} \right)^{\frac{1}{2}} \quad (7)$$

The experimental conditions and the kinetic results of the crystallization experiments in the absence of orthophosphate ions are summarized in Table 1.

In all crystal growth experiments, despite the fact that the solutions were supersaturated with respect to all calcium carbonate polymorphs as may be seen in Table 1, FTIR spectrum (Fig. 1a) and X-ray patterns (Fig. 1b) of the grown crystals remained identical to the ones of the aragonite seed crystals, which showed that the overgrown phase was exclusively aragonite. Aragonite crystallized as irregular and prismatic needles of about 5 μm in length and 1 μm width (Fig. 1c).

Mechanistic information concerning the rate determining step for crystal growth may be obtained from plots of the dependence of the rates of crystal growth of the mineral phase, R_g, *versus* the relative supersaturation. A simple semi-empirical power law equation may be used for the correlation of the crystal growth measured as a function of the corresponding supersaturation:

$$R_g = k_g \sigma^n \quad (8)$$

In Eq. (8), k_g is the apparent crystal growth rate constant, which is a function of the active growth sites on the seed crystals and *n* the apparent kinetic order. The value of *n* is indicative of the mechanism of crystal growth. Kinetics plots of the rates of crystal growth of aragonite on the aragonite seed crystals according to Eq. (8) are shown in Fig. 2.

Table 1
Experimental conditions and crystal growth rate (R_g) for the crystallization of aragonite on aragonite seed crystals in the absence of orthophosphate ions, in aqueous solutions at conditions of constant supersaturation: total calcium, Ca_T=total carbonate, C_T; pH 7.80 ± 0.10, T=37.0 ± 0.1 °C, ionic strength: 0.15 M in NaCl.

Ca_T (mM)	$\sigma_{vaterite}$	$\sigma_{aragonite}$	$\sigma_{calcite}$	R_g ($\times10^{-6}$ mol min^{-1} m^{-2})
4.5	0.17	0.86	1.14	4.3
5.0	0.46	1.32	1.66	11.5
5.5	0.53	1.43	1.78	14.0
6.0	0.66	1.63	2.02	19.1
6.5	0.74	1.75	2.16	23.0
7.0	0.84	1.92	2.35	27.4

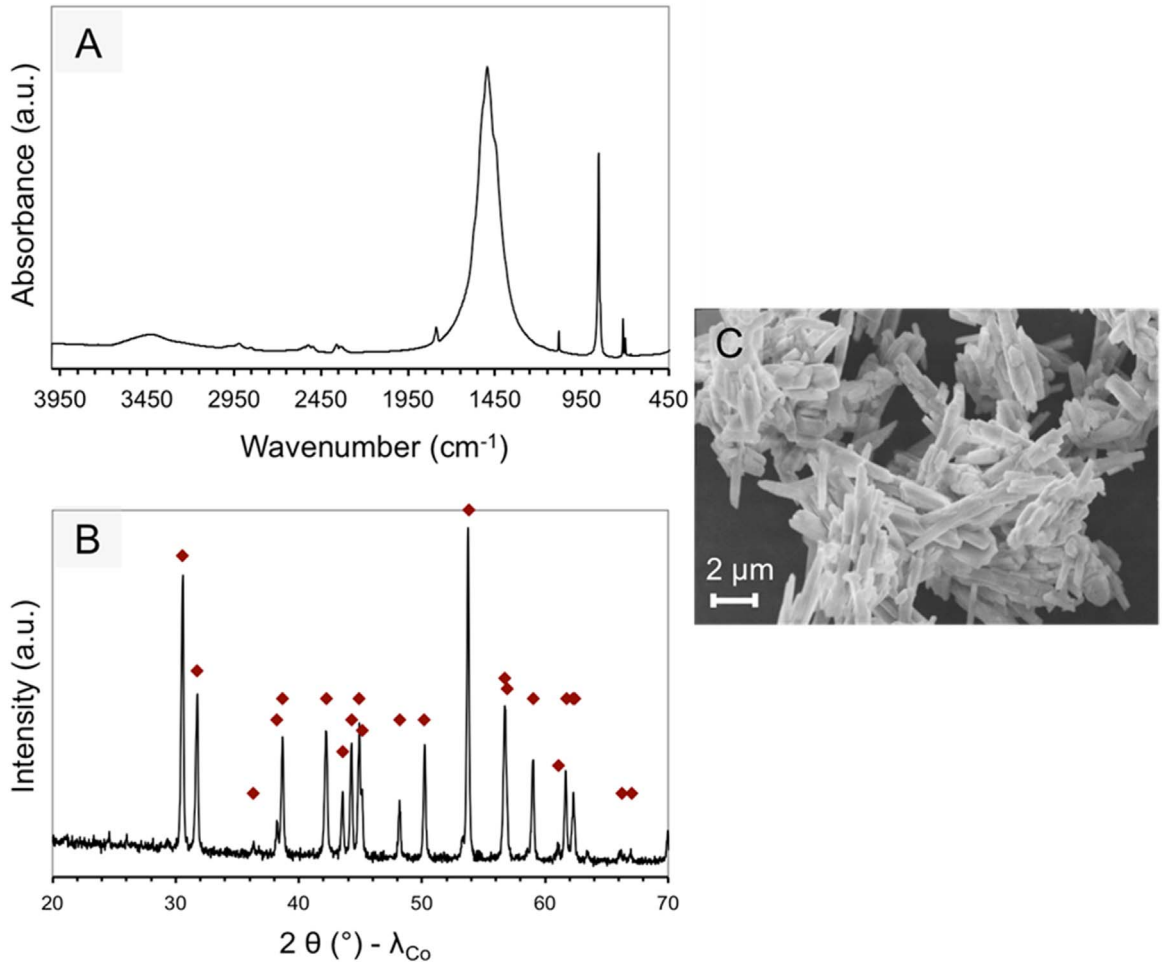

Fig. 1. Characteristics of aragonite crystals after crystal growth experiment at constant solution supersaturation and in absence of orthophosphate ions: FTIR spectrum (a), powder X-ray diffractogram (b, rhomboid symbols show the aragonite seeds diffraction peaks assigned in comparison with the JCPDS n° 411475 reference data) and SEM micrograph (c).

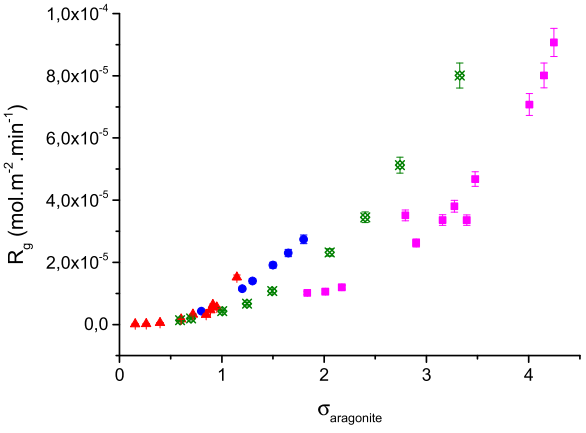

Fig. 2. Kinetics of seeded crystal growth of aragonite on aragonite seed crystals. Plot of the rate of crystal growth, R_g, as a function of the relative supersaturation with respect to aragonite for this study ((●)) at pH 7.8, 37 °C, 0.15 M NaCl and those reported in the literature: ((▲)) [31]; ((◆)) [11]; ((■)) [28].

The apparent kinetic order for the crystal growth of aragonite on calcium carbonate seed crystals was found to be n=2.2 ± 0.2. This result is in agreement with literature reports from crystal growth experiments of aragonite in seawater and at various salinities [11,28,31]. The calculated value for the apparent order of growth suggested that the growth of aragonite was controlled by surface diffusion.

3.2. Influence of the presence of low concentrations of orthophosphate ions on the crystallization of aragonite

The presence of inorganic orthophosphate ions in the supersaturated solutions at very low concentrations (0.25–10 µM), which did not significantly influence the supersaturation with regard to aragonite ($\sigma_{aragonite}$=1.75), had a significant impact on the aragonite seeded crystal growth rate (Table 2). The rate of crystal growth of aragonite was reduced by almost 95% in the presence of 7 µM of orthophosphate (Fig. 3). The inhibition percentage in the presence of orthophosphate

Table 2
Experimental conditions and results for the crystallization of aragonite on aragonite seed crystals (induction time, τ, and crystal growth rate, R_g) in the presence of orthophosphates in aqueous solutions at constant supersaturation ($\sigma_{aragonite}$=1.75): pH 7.80 ± 0.10, T=37.0 ± 0.1 °C, ionic strength: 0.15 M in NaCl.

$[C_{Phosphate}]$ (µM)	Induction time, τ (s)	σ_{HAP}	R_g ($\times 10^{-6}$ mol min^{-1} m^{-2})
0.00	–	–	23.0
0.25	–	1.02	20.9
0.50	–	1.55	17.6
1.00	–	2.22	14.4
2.00	25	3.05	7.9
2.50	30	3.36	5.8
3.00	35	3.63	3.6
5.00	90	4.40	2.1
7.00	240	5.14	1.2
10.00	∞	5.92	–

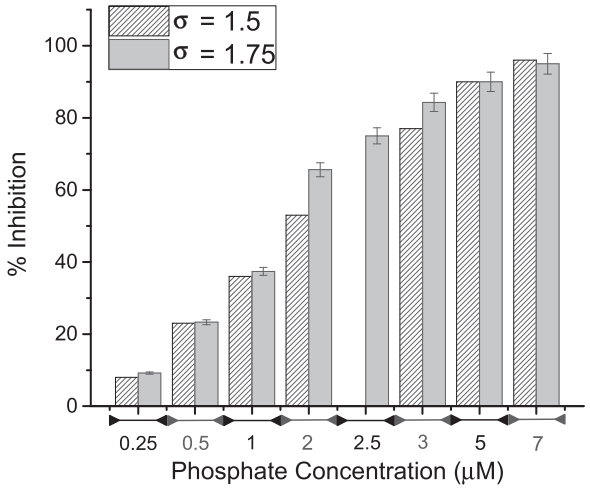

Fig. 3. Percentage of inhibition of the rates of crystal growth of aragonite on aragonite seed crystals as a function of the orthophosphate concentration in solution for two different supersaturations ($\sigma_{aragonite}$=1.5 and $\sigma_{aragonite}$=1.75) at pH 7.8, 37 °C and 0.15 M NaCl.

was calculated according to Eq. (9):

$$Inhibition\ (\%) = \frac{R_{g,0} - R_{g,i}}{R_{g,0}} \times 100 \quad (9)$$

where $R_{g,o}$, $R_{g,\,i}$ are the measured crystal growth rates in the absence and in the presence of orthophosphate in the supersaturated solution respectively. The degree of inhibition as a function of the orthophosphate concentration in the supersaturated solutions is shown in Fig. 3 for two different supersaturations ($\sigma_{aragonite}$=1.5 and $\sigma_{aragonite}$=1.75). Aragonite crystallization inhibition in the presence of orthophosphate was found not influenced by the relative supersaturation in the range of 1.5–1.75.

It is interesting to note that when orthophosphate concentration in the calcium carbonate supersaturated solution exceed 2.0 μM, measurable induction time periods were observed, preceding the onset of crystal growth of the aragonite seed crystals (Table 2). Since the solution supersaturation with respect to aragonite was not affected in the range of orthophosphate concentrations tested, it may be suggested that the presence of orthophosphate ions acted as both a nucleation and crystal growth inhibitor. The induction times, measured before the initiation of crystal growth, are considered to reflect the time needed for the formation of the critical nucleus and its increase to critical size. It should be noted that despite the fact that the solutions were supersaturated with respect to hydroxyapatite ($Ca_5(PO_4)_3OH$, HAP, see Table 2), this solid was not found in the precipitates. Longer induction times corresponded to solutions with the highest supersaturation with respect to HAP. The variation of the induction times *versus* the orthophosphate concentration in the supersaturated solutions is shown in Fig. 4.

It may be suggested that the inhibition of the crystal growth of aragonite is mainly due to the blockage of the active sites on the surface of aragonite. Atomistic studies have shown that there is specific selectivity for the adsorption of HPO_4^{2-} ions, prevalent at the pH of the solutions of the present work (7.8), for the {10-10} face of aragonite because of stereochemical control [32]. Solid state NMR measurements in corals grown in the presence of orthophosphate have also shown the uptake of phosphate ions present in defects and in apatitic inclusions, which were not found in the present work probably because of the relatively short time of contact between aragonite with the orthophosphate ions [33]. The presence of orthophosphate adsorbed onto the growing aragonite crystals was identified. The examination of the infrared spectra of the solids obtained from the crystallization of aragonite on the aragonite seed crystals at conditions of constant

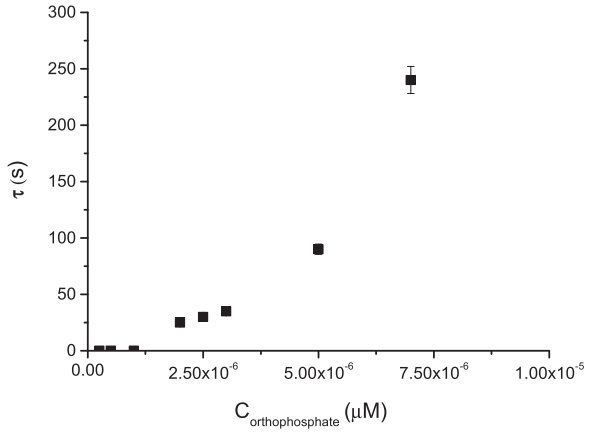

Fig. 4. Crystal growth of aragonite on aragonite seed crystals. Induction times, τ, preceding the initiation of crystal growth as a function of the orthophosphate concentration in solution (pH 7.80 ± 0.10, T=37.0 ± 0.1 °C, ionic strength: 0.15 M in NaCl, $\sigma_{aragonite}$=1.75).

supersaturation in the absence and presence of orthophosphate ions showed the presence of the characteristic bands of aragonite without the presence of additional bands characteristic to orthophosphate adsorption i.e υ_2 at 856 cm^{-1}, υ_4 at 713 cm^{-1} and υ_3 at 1490 cm^{-1} [34]. Considering the observation of adsorption, the lack of characteristic orthophosphate bands may be attributed to the fact that the amount adsorbed was low and under the detection limit of the technique. It also served as proof that no calcium phosphate was precipitated on the surface of aragonite. The adsorption of orthophosphate on the aragonite seed crystals was investigated independently of the crystal growth experiments through the construction of the respective adsorption isotherms.

3.3. Adsorption experiments

To investigate deeper the effect of orthophosphate ions in the concentration range 0.25–10 μM, adsorption experiments were performed on aragonite seeds. The surface concentration of the adsorbed phosphate, Γ (measured as total phosphate), was calculated from Eq. (10):

$$\Gamma = \frac{(c_0 - c_{eq})V}{mS} \quad (10)$$

where c_o, c_{eq} are the initial and equilibrium concentrations, respectively, V the volume of suspension, m the mass of the suspended crystals of aragonite and S their specific surface area.

The measured adsorption data are reported in Fig. 5.

As may be seen from Fig. 5, there is no dependence of the

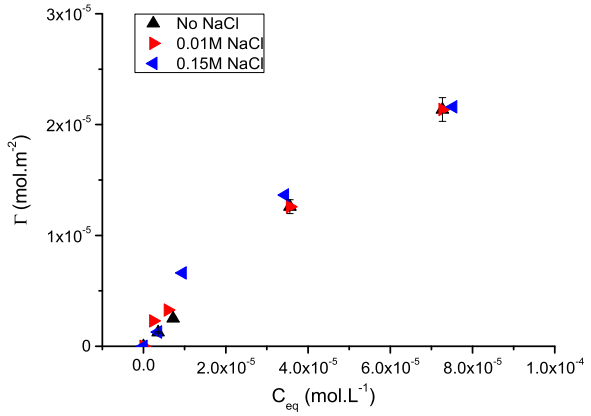

Fig. 5. Adsorption isotherm of orthophosphate on aragonite seed crystals at different ionic strength values; initial pH=8.2, 37 °C.

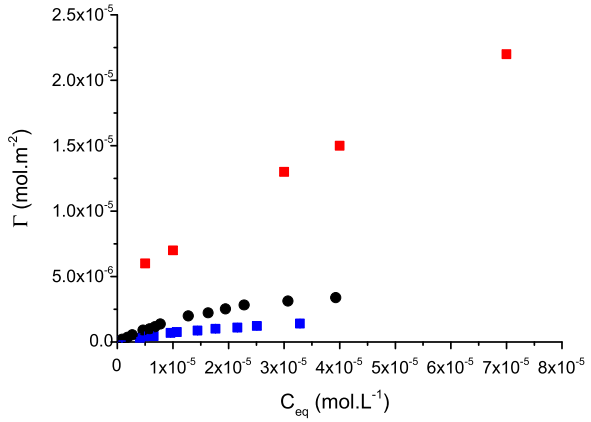

Fig. 6. Adsorption isotherm of orthophosphate on aragonite seed crystals at different ionic strengths and temperatures: ((■)) present work, initial pH 8.2, 37 °C, ionic strength 0.15 M; (•) Millero et al. pH 7.8, seawater (ionic strength 0.6 M), at 35 °C [0] and ((■)) at 25 °C [16].

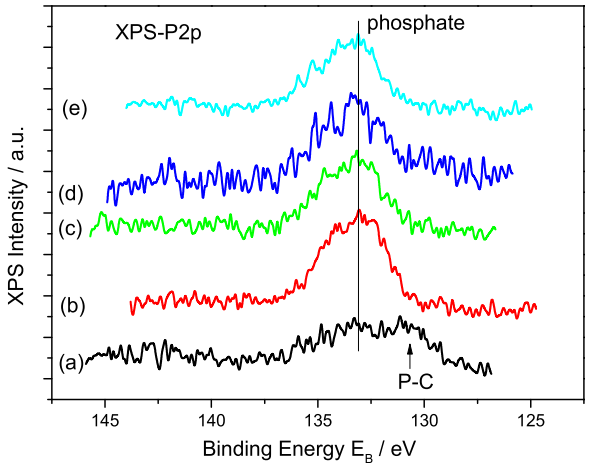

Fig. 7. XPS spectra of aragonite crystals equilibrated with orthophosphate solutions. (a) blank (b) 1.3 μmol m^{-2} (c) 6.6 μmol m^{-2} (d) 13.6 μmol m^{-2} (e) 21.6 μmol m^{-2}.

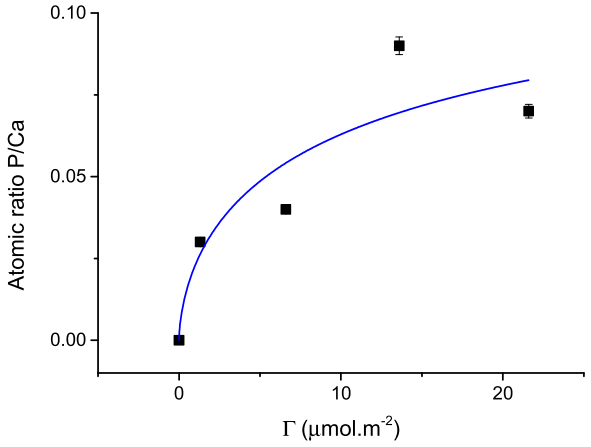

Fig. 8. Plot of the P/Ca atomic ratio evaluated from XPS data of aragonite seed crystals following adsorption of orthophosphate at 25 °C, 0.15 M NaCl, initial pH 8.2.

adsorption behavior on the ionic strength over the examined concentration range, a fact suggesting that the contribution of electrostatic forces on adsorption is relatively low, in agreement to suggestions by Reddy [17]. Assuming that the total surface area of a PO_4 group is 27.53 $Å^2$ [35] and the projection of one face of the PO_4 tetrahedron on a plane, using bond lengths to estimate the area, it was calculated that 0.28 μmol of orthophosphate are needed for a monolayer covering the

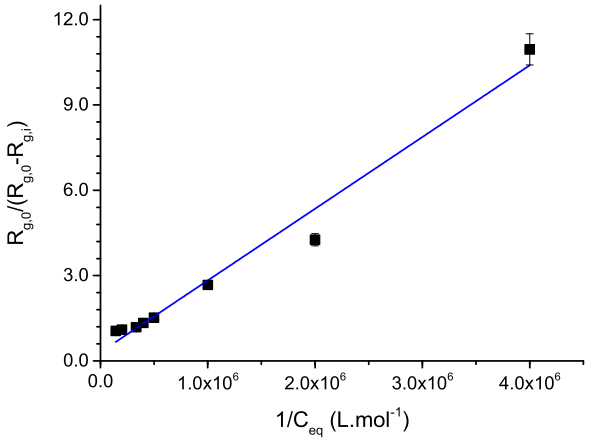

Fig. 9. Plot according to Eq. (14) for the crystal growth of aragonite on aragonite seed crystals in the presence of inorganic orthophosphate as a function of the equilibrium concentration of orthophosphate ions in the supersaturated solutions (pH 7.8, 37 °C).

aragonite seeds. In contrast with this calculation, the data plotted in Fig. 5 suggest that adsorption exceeded this amount by far. The excessive adsorption of orthophosphate ions on the aragonite surfaces may be responsible for the slow conversion of calcium carbonates into calcium phosphates by diffusion and substitution into the crystal matrix of the substrate [36], or by a dissolution-precipitation mechanism [37]. However extension of the ionic strength to that corresponding to seawater (~0.6 M) presented in the literature showed suppression of the adsorption, as may be seen in Fig. 6. The literature data have been replotted and expressed per unit surface area. The lower phosphate adsorption has been attributed by Millero et al. [16] to the competition of bicarbonate ions for adsorption onto aragonite. As may be seen in Fig. 6, our results are in agreement with the literature in which it is suggested that in seawater (high ionic strength) phosphate adsorption is suppressed even in the absence of magnesium and other ions forming strong complexes with the orthophosphate ions.

The solid residues of aragonite were washed repeatedly with a solution saturated with respect to aragonite and were dried overnight at 40 °C. The dry crystals were examined by powder X-ray diffraction and by FTIR spectroscopy. There was no evidence of adsorbed species or of any mineral phase, which would be indicated by the presence of additional reflections in the XRD patterns and/or bands on the FTIR spectra. Further analysis of the aragonite surfaces equilibrated with orthophosphate was done using XPS in order to analyze the very first surface layers of the aragonite crystals. The results of the XPS analyses are shown in Fig. 7.

As may be seen in Fig. 7, the P 2p spectra show a peak corresponding to the emission energy of adsorbed orthophosphate ions [38]. The broad band shown in the blank specimen is in the level of noise and it was taken as background. From the spectra the estimated P concentration on the surface showed a trend that was in agreement with the determinations from the adsorption isotherm. As may be seen in Fig. 8, the calculated P/Ca atomic ratio from the XPS data, corrected for the background spectrum showed a trend similar to the adsorption isotherm (Fig. 5), suggesting that there could be a limiting value for orthophosphate uptake on the surface of the aragonite seed crystals.

The calculation of orthophosphate uptake data, shown in Fig. 5, with one of the established thermodynamic models can only be done provided that adsorption is reversible. Phosphate analysis after the end of the reversibility of adsorption experiment showed that, in all cases, 10–12% of the adsorbed orthophosphate was desorbed. This extent of desorption is in agreement with literature results [39]. The adsorption data were fitted according to the Langmuir model:

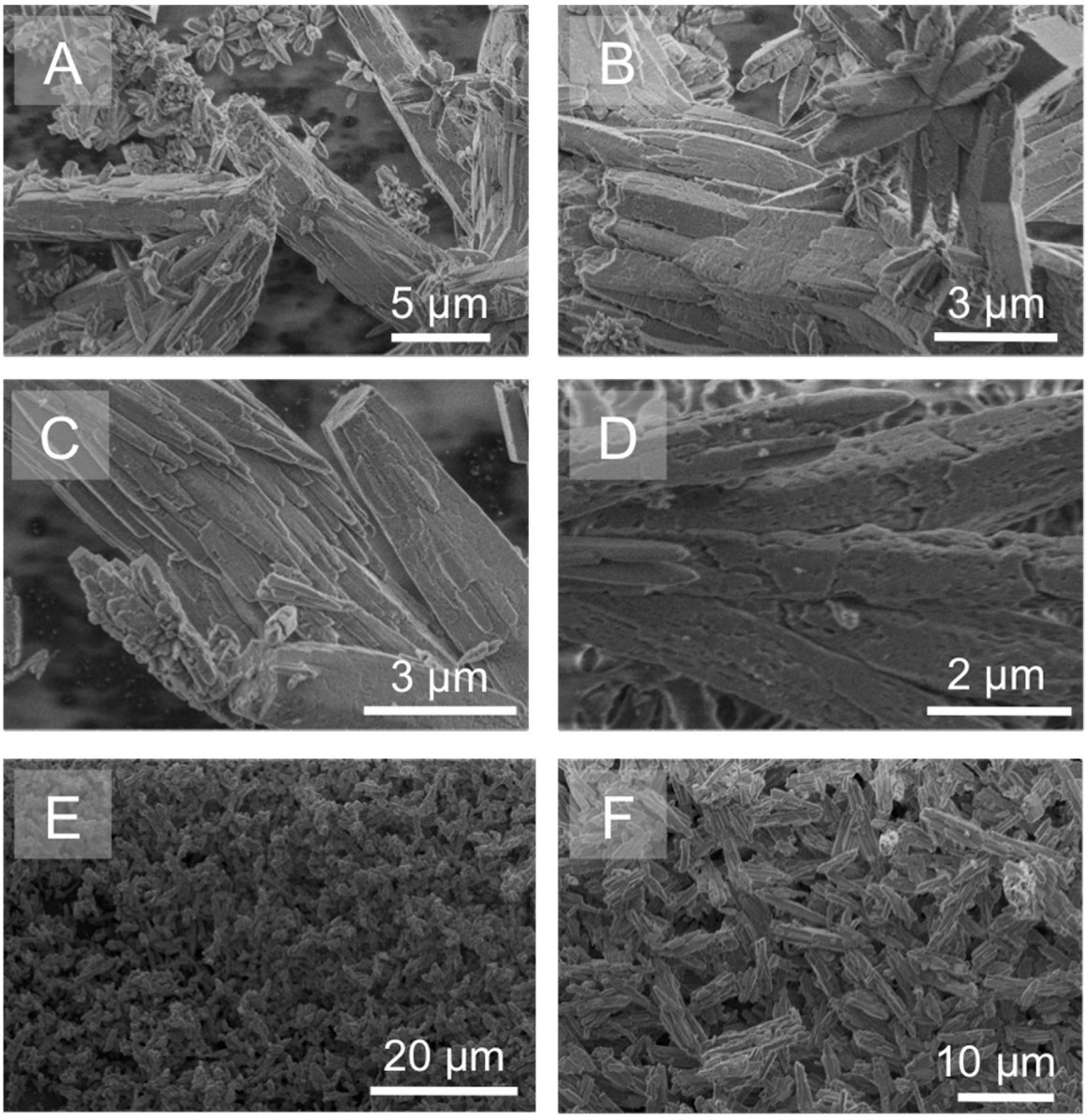

Fig. 10. SEM micrographs of aragonite crystals grown on aragonite seed crystals in the presence of orthophosphate (pH 7.8, 0.15 M NaCl, 37 °C) or equilibrated with orthophosphate ions (pH 8.2, 0.15 M NaCl, 25 °C): a,b: Aragonite seed crystals; c,d: Aragonite grown on aragonite seed crystals in the presence of 1 and 8 μM orthophosphate, respectively; e,f: Aragonite seed crystals after equilibration with 30 μM and 100 μM of orthophosphate solution, respectively.

$$\frac{C_{eq}}{\Gamma} = \frac{1}{\Gamma_m K_m} + \frac{C_{eq}}{\Gamma_m} \tag{11}$$

where Γ_m is the orthophosphate concentration corresponding to monolayer coverage and K_m is a parameter related to the energy of adsorption. From the plot according to Eq. (10) and from the linear fit of the data (r^2=0.96), a value of 29 μmol m^{-2} was calculated for the monolayer coverage. This value is fourfold higher than the value calculated from simple calculations based on the assumption of the dimensions of each PO_4 tetrahedral unit. This finding seems quite reasonable given the various modes of adsorption of tetrahedral orthophosphate on the aragonite surface.

Another way to consider phosphate uptake on aragonite crystal surface is based on the hypothesis of an ionic exchange carbonate/hydrogenphosphate. This phenomenon has been demonstrated in the case of carbonate uptake on calcium phosphate apatite [40]. In the present work, we could consider the exchange of carbonate ions from the aragonite crystals with the hydrogen phosphate from the solution following the chemical reaction:

$$CO^{2-}_{3(arag.)} + HPO^{2-}_{4(sol)} \leftrightarrow HPO^{2-}_{4(arag.)} + CO^{2-}_{3(sol)} \tag{12}$$

Examination of both the XPS spectra and the adsorption isotherm data, showed that orthophosphate ions adsorb onto the aragonite crystal surfaces, thus blocking the active growth sites. Considering that θ, the fraction of the active sites occupied by the orthophosphate ions is expressed as Eq. (13),

$$\theta = \frac{\Gamma}{\Gamma_m} \tag{13}$$

the rate of crystal growth, in the presence of orthophosphate, $R_{g,\,i}$, is expected to be lower than in its absence by a factor proportional to the surface coverage (Eq. (14)):

$$R_{g,i} = R_{g,0} - \theta(1-b)R_{g,0} \tag{14}$$

where b is a necessary constant ($0 \le b \le 1$) necessary to account for the fact that the rate is not fully suppressed even at coverages of the surface of the seeds equal or greater to those corresponding to monolayer coverage. The combination of Eqs. (10, 11 and 13) yields an expression

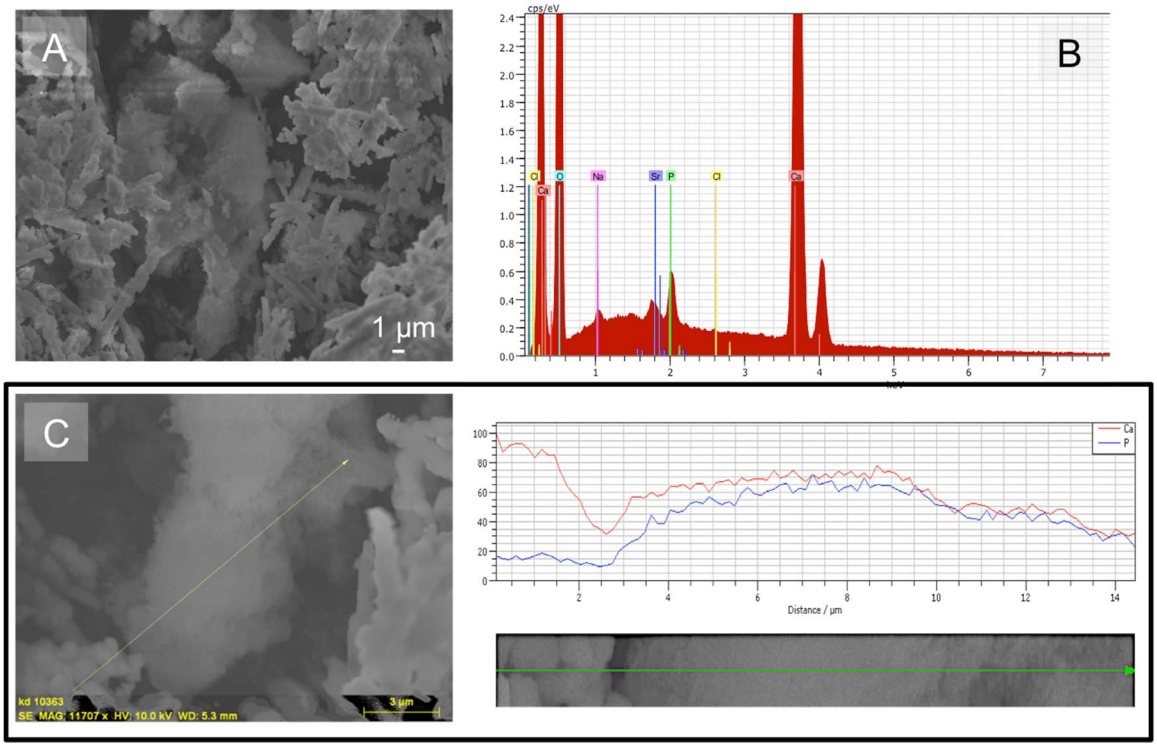

Fig. 11. Calcium phosphate grown on aragonite seed crystals under the conditions of σ=1.75 with respect to aragonite in the presence of 0.5 mM phosphate, 37 °C, 0.15 M NaCl, pH 7.8. a: SEM micrograph of the calcium phosphate precipitated (center of picture). b: EDX spectrum of the sample. c: Line scan showing the domain of calcium phosphate formation (SEM micrograph combined with EDX analysis).

correlating the rates of crystal growth in the absence and in the presence of inorganic orthophosphate ions with the equilibrium concentration [41]:

$$\frac{R_{g,0}}{R_{g,0} - R_{g,i}} = \frac{1}{1-b} + \frac{1}{(1-b)K_{aff}}\frac{1}{C_{eq}} \quad (15)$$

In Eq. (15) K_{aff} is a constant indicative of the affinity between the adsorbate and the adsorbent. In the ideal Langmuir type behavior (b=0), full coverage with a monolayer (θ=1) is expected to entirely inhibit the rate of crystal growth. If the intercept of the line described by Eq. (15), is >1, the inhibitor is unable to suppress crystal growth rates even at surface coverage equal to and/or greater than the corresponding to monolayer coverage. If the intercept is <1, complete suppression of the crystal growth rates may be achieved below monolayer coverage of the surface of the growing crystals [42]. The plot according to Eq. (15) and a linear fit of the data is shown in Fig. 9.

From the slope of the line of best fit to the experimental data, a value of K_{aff}≈4×10^5 L mol^{-1} was calculated, which is in good agreement with literature values for calcium carbonate, suggesting a strong interaction between aragonite and orthophosphate ions [43]. The value of the intercept of the linear plot was 0.31, suggesting complete inhibition of the crystal growth at a surface coverage below that corresponding to the formation of a monolayer of orthophosphate.

The morphology of the crystals grown in the absence and in the presence of orthophosphate in the supersaturated solutions is shown in the SEM micrographs (Fig. 10). As may be seen, there were no changes in the morphology of the crystals and the particle size was affected to the extent that crystal growth took place. Since growth was seeded, growth took place exclusively on the inoculating seed crystals.

3.4. Influence of the presence of higher concentrations of orthophosphate ions on the crystallization of aragonite

As may be seen in Fig. 10, the presence of orthophosphate did not affect the morphology of the aragonite crystals either grown at conditions of constant supersaturation (Fig. 10c and d) or in saturated solutions in the presence of suspended aragonite seed crystals (adsorption experiments, Fig. 10e and f). Raising the concentration of orthophosphate in the supersaturated solutions to levels as high as 0.5 mM and 1 mM (*i.e.* closer to that in blood plasma) resulted in the co-precipitation of calcium phosphate with aragonite as may be seen in Fig. 11, which shows the morphology of the crystals formed (Fig. 11a and c) and the corresponding microanalysis results (Fig. 11b and c). However, the precipitation at these concentration levels was rather non-specific and did not take place at constant supersaturation, which is the reason why the influence of such a high orthophosphate concentration was not further studied.

The calcium phosphate phase may be seen in the in the central part of Fig. 11a and the overall EDX spectrum of the sample clearly shows the presence of calcium phosphate. It should be noted that in the presence of a total orthophosphate concentration below 50 µM in the supersaturated solutions, no phosphate peak was observed. At concentrations higher than 0.5 mM of phosphate, the solution was supersaturated with respect to all calcium phosphate phases and the driving force was sufficiently high to overcome the barrier for the formation of calcium phosphate.

4. Conclusions

We report for the first time the crystal growth of aragonite at constant solution supersaturation and pH and temperature close to physiological conditions. The presence of orthophosphate ions, in the range between 1–8 µM, in solutions supersaturated with respect to all calcium carbonate phases was found to reduce the rate of crystal growth of aragonite at pH 7.8 and 37 °C. The rates of crystal growth were measured with the seeded growth technique under conditions of constant supersaturation. For phosphate concentrations in solution in the range of 2–7 µM, induction times were measured, suggesting that in this range of concentrations nucleation was inhibited as well. At concentration levels exceeding 8 µM the presence of orthophosphate

completely suppressed the crystal growth of aragonite. The results of the kinetics measurements suggested that the inhibition of aragonite crystal growth is due to the adsorption of orthophosphate onto the active growth sites of the seed crystals. Adsorption studies showed that electrostatic interactions at ionic strength values < 0.15 M play a rather minor role in the uptake mechanism and the adsorption data were fitted satisfactorily to the Langmuir model. XPS analyses confirmed the presence of inorganic orthophosphate on aragonite without the formation of surface crystalline layers of calcium phosphates or in quantities too low to be detected by other characterization means (EDX, FTIR spectroscopy). Finally, the presence of orthophosphate in solutions (up to 0.5 mM) either at equilibrium with aragonite or in supersaturated solutions (up to 8 μM) did not affect the morphology of the aragonite crystals. At 0.5 mM of orthophosphate and above, calcium phosphate precipitated, thus rendering it impossible to maintain a constant composition in the solution.

These fundamental results obtained *in vitro* contribute to the understanding of the role of orthophosphate in biological fluids can have on the behavior of aragonite-based biomaterials once implanted *in vivo*. In particular, for calcium carbonate-based bone cements, their *in vivo* setting reaction, evolution and resorption behavior will most probably be impacted by the presence of orthophosphate ions.

Acknowledgments

The authors thank the Institut National Polytechnique de Toulouse (France) for supporting this bilateral work (BQR SMI). We would like to acknowledge the help by Dr. Lambrini Syggelou for the XPS spectra and calculations. Partial support of the work by the European Union (European Social Fund-ESF) and Greek National Funds through the Operational program "Education and Lifelong Learning" under the action Aristeia II (Code No 4420, contract # 1111/31-01-2014).

References

[1] J.W. Morse, R.S. Arvidson, A. Lüttge, Calcium carbonate formation and dissolution, Chem. Rev. 107 (2007) 342–381.
[2] N.K. Dhami, M.S. Reddy, A. Mukherjee, Biomineralization of calcium carbonates and their engineered applications: a review., Front. Microbiol. 4 (2013) 13.
[3] K.J. Westin, A.C. Rasmusson, Crystal growth of aragonite and calcite in the presence of citric acid, DTPA, EDTA and pyromellitic acid, J. Colloid Interface Sci. 282 (2005) 359–369.
[4] A. Zieba, G. Sethuraman, F. Perez, G.H. Nancollas, D. Cameron, Influence of organic phosphonates on hydroxyapatite crystal growth kinetics, Langmuir 12 (11) (1996) 2853–2858.
[5] B.N. Bachra, O.R. Trautz, S.L. Simon, Precipitation of calcium carbonates and phosphates. I. Spontaneous Precipitation of calcium carbonates and phosphates under physiological conditions, Arch. Biochem. Biophys. 103 (1963) 124–138.
[6] W.A. House, Inhibition of calcite crystal growth by inorganic phosphate, J. Colloid Interface Sci. 119 (1987) 505–511.
[7] A. Katsifaras, N. Spanos, Effect of inorganic phosphate ions on the spontaneous precipitation of vaterite and on the transformation of vaterite to calcite, J. Cryst. Growth 204 (1999) 183–190.
[8] Th.G. Sabbides, P.G. Koutsoukos, The effect of surface treatment with inorganic orthophosphate on the dissolution of calcium carbonate, J. Cryst. Growth 165 (1996) 268–272.
[9] Y.B. Hu, M. Wolthers, D.A. Wolf-Gladrow, G. Nehrke, Effect of pH and phosphate on calcium carbonate polymorphs precipitated at near freezing temperature, Cryst. Growth Des. 15 (2015) 1596–1601.
[10] J. De Kanel, J.W. Morse, The chemistry of orthophosphate uptake from seawater onto calcite and aragonite, Geochim. Cosmochim. Acta 42 (1978) 1335–1340.
[11] E.A. Burton, L.M. Walter, The role of pH in phosphate inhibition of calcite and aragonite precipitation rates in seawater, Geochim. Cosmochim. Acta 54 (1990) 797–808.
[12] N. Xu, Y. Wang, X. Xu, C. Liu, J. Qian, G. Feng, Mechanisms and applications of the synthesized fusiform aragonite for the removal of high concentration of phosphate, Water Air Soil Pollut. 64 (2016) 227.
[13] W.A. House, L. Donaldson, Adsorption and coprecipitation of phosphate on calcite, J. Colloid Interface Sci. 112 (1986) 309–324.
[14] H.U. So, D. Postma, R. Jakobsen, F. Larsen, Sorption of phosphate onto calcite; results from batch experiments and surface complexation modeling, Geochim. Et. Cosmochim. Acta 75 (2011) 2911–2923.
[15] W. Stumm, J.O. Leckie, Phosphate exchange with sediments: its role in the productivity of surface water, Advances in Water Pollution Research, Part III 2, Pergamon Press, New YorK, 1970, pp. 26/1–26/16.
[16] F. Millero, F. Huang, X. Zhu, X. Liu, J.Z. Zhang, Adsorption and desorption of phosphate on calcite and aragonite in seawater, Aq. Geochem 7 (2001) 33–56.
[17] M.M. Reddy, Crystallization of calcium carbonate in the presence of trace concentrations of phosphate containing anions. I. Inhibition by phosphate and glycerophosphate ions at pH 8.8 and 25 °C, J. Cryst. Growth 41 (1977) 287–295.
[18] P. Ducheyne, K. Healy, D.E. Hutmacher, D.W. Grainger, C.J. Kirkpatrick, Comprehensive Biomaterials, Boston 217, Elsevier, Amsterdam, 2011.
[19] S.A. Hamid, A.R. Samsudin, R. Salim, N. Omar, Coral as bone graft substitute, in: A. Nather (Ed.)Bone Grafts and Bone Substitutes: Basic Science and Clinical Applications, World Scientific Publ, New Jersey, London, Co, 2005, pp. 533–546.
[20] M.L. Fontaine, C. Combes, T. Sillam, G. Dechambre, C. Rey, New calcium-carbonate-based cements for bone reconstruction., Key Eng. Mater. 284–286 (2005) 105–108.
[21] C. Combes, B. Miao, R. Bareille, C. Rey, Preparation, physical chemical characterisation and cytocompatibility evaluation of calcium carbonate cements, Biomaterials 27 (2006) 1945–1954.
[22] M.L. Fontaine, C. Combes, S. Mounic, C. Rey, Composition de ciment hydraulique à base de carbonates de calcium, Patent No. FR2830249, 2001.
[23] R. González, N. Merino, P. Rodríguez, V.M. Rodríguez, In vivo transformation of a calcium carbonate (aragonite) based implants biomaterial to bone. A histological, chemical and FT-IR study, Rev. CENIC Cienc. Biológicas 35 (2004) 7–13.
[24] S.A. Redey, S. Razzouk, C. Rey, D. Bernache-Assollant, G. Leroy, M. Nardin, G. Cournot, Osteoclast adhesion and activity on synthetic hydroxyapatite, carbonated hydroxyapatite, and natural calcium carbonate: relationship to surface energies., J. Biomed. Mater. Res. 45 (1999) 140–147.
[25] E. Busenberg, L.N. Plummer, A comparative study of the dissolution and crystal growth kinetics of calcite and aragonite, Studies in diagenesis 1578, US Geol Surv Bull, Washington DC, 1986, pp. 139–168.
[26] L.M. Walter, LM, Relative efficiency of carbonate dissolution and precipitation during diagenesis: a progress report on the role of solution chemistry: roles of organic matter in mineral diagenesis, in: D.L. Gautier (Ed.), Soc. Econ. Paleon. Mineralogists Spec. Pub. 38 (1986), 1986, pp. 1–11.
[27] E.A. Burton, L.M. Walter, Relative precipitation rates of aragonite and Mg calcite from seawater - Temperature or carbonate ion control, Geology 15 (1987) 111–114.
[28] C.S. Romanek, J.W. Morse, E.L. Grossman, Aragonite kinetics in dilute solutions, Aquat. Geochem. 17 (2011) 339–356.
[29] Z.R. Hinedi, S. Golberg, A.C. Chang, J.P. Yesinowski, A ^{31}P and ^{1}H MAS NMR study of phosphate sorption on calcium carbonate, J. Colloid Interface Sci. 152 (1991) 141–160.
[30] D.L. Parkhurst, C.A.J. Appelo, Description of input and examples for PHREEQC version 3 - A computer program for speciation, batch- reaction, one-dimensional transport, and inverse geochemical calculations: u.s. Geological Survey. chap A43Tech. Methods, Book 6 497 (2013) [Available only at] ⟨http://pubs.usgs.gov/tm/06/a43⟩.
[31] S. Zhong, A. Mucci, Calcite and aragonite precipitation from seawater solutions of various salinities: precipitation rates and overgrowth compositions, Chem. Geol. 78 (1989) 283–299.
[32] J.O. Titiloye, S.C. Parker, S. Mann, Atomistic simulation of calcite surfaces and the influence of growth additives on their morphology, J. Cryst. Growth 131 (1993) 533–545.
[33] H.E. Mason, P. Montagne, L. Kibista, M. Taviani, M. McCulloch, B.L. Phillips, Phosphate defects and apatite inclusions in coral skeletal aragonite revealed by solid state NMR spectroscopy, Geochim. Cosmochim. Acta 75 (2011) 7446–7457.
[34] Z. Zhang, Y. Xie, X. Xu, H. Pan, R. Tang, Transformation of amorphous calcium carbonate into aragonite, J. Cryst. Growth 343 (2012) 62–67.
[35] A.S. Posner, A. Perloff, Apatites deficient in divalent cations, J. Res. Nat. Bur. Stand. 58 (1957) 279–286.
[36] J.G. Dunn, P.W. Sammarco, G. LaFleur Jr., Effects of phosphate on growth and skeletal density in the scleractinian coral Acropora muricata: a controlled experimental approach, J. Exp. Mar. Biol. Ecol. 411 (2012) 34–44.
[37] A. Kasioptas, T. Geisler, C.V. Putnis, C. Perdikouri, A. Putnis, Crystal growth of apatite by replacement of an aragonite precursor, J. Cryst. Growth 312 (2010) 2431–2440.
[38] M. Soma, H. Seyama, X-Ray Photoelectron spectroscopy study of the surface composition of sediment or soil models, Appl. Surf. Sci. 8 (1981) 478–482.
[39] Q. Wang, Y. Li, Phosphorus adsorption and desorption behavior on sediments of different origins, J. Soils Sediment. 10 (2010) 1159–1173.
[40] C. Rey, C. Combes, C. Drouet, S. Cazalbou, D. Grossin, F. Brouillet, S. Sarda, Surface properties of biomimetic nanocrystalline apatites: application in biomaterials, Prog. Cryst. Growth Charact. Mater. 60 (2014) 63–73.
[41] N. Spanos, P.G. Koutsoukos, Model studies of the effect of orthophospho-L-serine on biological mineralization, Langmuir 17 (2001) 866–872.
[42] G.H. Nancollas, S.J. Zawacki, Industrial Crystallization, in: S.J. Jancic, E.J. DeJong (Eds.), , Elsevier Science Publ. Amsterdam 84 (1984), 1984.
[43] Z. Amjad, Kinetic study of the seeded growth of calcium carbonate in the presence of benzenepolycarboxylic acids, Langmuir 3 (1987) 224–228.